Available online at www.sciencedirect.com
SCIENCE DIRECT®
Journal of Sound and Vibration 293 (2006) 59–77
JOURNAL OF SOUND AND VIBRATION
www.elsevier.com/locate/jsvi

Linear control strategies for damping of flexible structures

Jan R. Høgsberg*, Steen Krenk

Department of Mechanical Engineering, Technical University of Denmark, Building 403, DK-2800 Kgs. Lyngby, Denmark

Received 9 May 2005; received in revised form 10 September 2005; accepted 21 September 2005
Available online 18 November 2005

Abstract

Starting from the two-component representation technique for damping of structures the possible increase in damping efficiency obtained by introducing collocated active damping is illustrated. The two-component representation of the damped vibration mode is constructed as a linear combination of the undamped mode shape and the mode shape obtained by locking the damper. This leads to a simple set of equations of motion, which in the frequency domain gives an accurate solution for the complex-valued natural frequency, and thereby for the modal damping. This solution shows that attainable damping increases with the phase angle of the damper, and that improved damping efficiency thus follows from the ability of an active device to produce a force acting ahead of velocity. Phase lead is equivalent to negative stiffness, and the effect of negative stiffness is illustrated by a radiation condition on a cable. Simple linear filters, with desirable low-pass properties, are presented as simple means for implementing phase lead.

1. Introduction

The internal damping in flexible structures is often so small that additional energy dissipation is needed in the form of external dampers. The tuning of a damper is crucial, because too little damping leaves the structure insufficiently damped, while too much damping clamps the damper and restrains the structure at the location of the damper with virtually no damping effect. In general, external dampers can be classified as being either passive or active. Passive damping produces entirely dissipative forces, and is typically autonomous and collocated. It follows from these properties that it is stable under any circumstances. Passive damping is similar to material damping, where the effective damping force may have frequency components in phase with the displacement (strain) and velocity (strain rate). The component in phase with the displacement has the character of an increased stiffness. A review of the most common passive devices, such as viscous and viscoelastic dampers or tuned mass and liquid dampers, has been given in Ref. [1]. Active damping, on the other hand, may rely on non-collocated sensor–actuator systems and can produce non-dissipative forces. Thus, active damping does not necessarily guarantee stability. Active damping is often based directly or via approximations on the results from linear optimal control, where the damper forces are optimized with respect to minimization of a weighted cost functional, see e.g. Ref. [2]. The tuning of this control usually relies on a pole-placement technique, where the closed-loop poles of a limited number of structural modes are located in

*Corresponding author. Tel.: +45 4525 1971; fax: +45 4588 4325.
E-mail addresses: jhg@mek.dtu.dk (J.R. Høgsberg), sk@mek.dtu.dk (S. Krenk).

0022-460X/$ - see front matter © 2005 Elsevier Ltd. All rights reserved.
doi:10.1016/j.jsv.2005.09.014

the complex plane according to some design criteria. The efficiency and stability of this approach depends on a sufficiently detailed and accurate description of the underlying structural model, in particular if an observer filter is present. Therefore, the possible energy spill-over into modes outside the truncated model and general uncertainties in the model parameters may lead to uncontrolled modes, that in some cases can be attenuated or even destabilized, e.g. as noted in Ref. [3].

The goal of structural damping is to reduce the magnitude of the response. For harmonic resonant response the response magnitude is inversely proportional to the damping ratio, while it is less directly related to the dissipated energy. For this reason the damping ratio ζ—and not, e.g. the absolute damping $\zeta\omega$—is used to characterize the quality of damping in the following. Collocated active control constitutes an attractive means for damping of flexible structures. The active nature of the control enables adjustment to the actual motion of the structure, and the collocated nature of the sensor–actuator system reduces the dependence on accurate system models. When assuming perfect actuator dynamics it can be shown that a collocated sensor–actuator configuration leads to guaranteed stability, see e.g. Ref. [4]. This implies a limitation of the potential energy spill-over to higher modes. Collocated active control has been widely used for damping of flexible structures, such as large space trusses [5], cables [6], and cable-stayed bridges [7]. Energy dissipation requires a force component in phase with velocity. Thus, the simplest linear model is direct velocity feedback [5], which appears as an active realization of pure viscous damping. Additional flexibility might be obtained by introducing various filter models based on feedback of either position [8], acceleration [9], or force [4], respectively. An extensive review of collocated control has been given in Ref. [4].

The present analysis considers the effect of a linear collocated damper, acting on a discretized structural model, where the governing equations of motion are typically formulated as a finite element model. The damping efficiency is evaluated in terms of the modal properties of the system. The damper is linear and collocated, and the steady-state properties are thus effectively characterized in the frequency domain via a damper gain and a complex-valued transfer function, relating the energy conjugated force and displacement amplitudes. This transfer function is represented by phase angle and magnitude, whereby a phase angle equal to $\pi/2$ corresponds to viscous damping fully in phase with velocity, whereas a phase angle less, or larger, than $\pi/2$ corresponds to a damper force acting behind, or ahead of, velocity, respectively.

The use of modal damping for flexible structures requires identification of a representative mode including the effect of the damper. Traditional reduction techniques for non-classically damped systems rely on one of the following two approaches. The first approach uses the undamped mode shapes and omits any non-zero off-diagonal terms in the corresponding modal damping matrix. This truncation is asymptotically correct in the limit of vanishing gain [10]. However, for large damping it neglects important coupling effects between the various undamped modes due to the presence of the damper. The other approach is based on a decomposition in terms of the complex-valued mode shapes obtained from the equations of motion formulated in state–space. This approach relies on the solution of an eigenvalue problem of double size, which in many cases is undesirable, and in addition the complex mode shapes depend on the magnitude of the damping.

The present paper adopts a new reduction technique introduced by Main and Krenk [11], where the reduced set of dynamic equations are found by a projection on to the subspace expanded by the undamped mode shape and the mode shape arising when clamping the damper and thereby locking the structure at the location of the damper. This representation is exact in the limits of zero and infinite gain. The problem of optimal damping is hereby reduced to a system with two degrees of freedom, for which a fairly simple, yet accurate, solution can be found. This approach is superior to the classical approach, where a relatively large number of undamped modes is needed to give a sufficiently accurate representation of the damped modes. A procedure leading to similar expressions has been derived in Ref. [4] via a diagonalization technique where coupling effects are neglected. Accurate asymptotic solutions in the same format have previously been derived for viscous dampers attached to various continuous systems such as a taut cable [12], a cable with sag [13], or a simply supported beam [14]. An important point of the present paper is to demonstrate the accuracy of the system reduction technique in active damping of flexible structures.

In the frequency domain, where the effect of the damper is represented by the transfer function, this leads to a determinant equation with a quartic characteristic polynomial in the natural frequency. This equation is conveniently rewritten into an implicit format that is suitable for numerical solution for given damper properties. When coupling effects between the undamped and the infinitely damped mode shapes are

neglected, this expression gives an explicit relation between the natural frequency and the damper properties. Despite the approximate nature of this format it gives a clear interpretation of the effect of the viscosity and stiffness of the damper, as illustrated by an example, where ideal energy radiation in a cable is realized by a combination of an impedance condition and a significant negative stiffness component.

In general terms the combined effects of stiffness and viscosity are related via the phase angle of the transfer function. The influence of the phase angle has been analyzed in Ref. [15] in terms of the so-called fractional derivative model. This analysis shows that attainable damping increases with phase angle, and that active damping thus is superior to passive damping due to its ability to generate a control force acting ahead of velocity.

Since fractional derivatives are difficult to realized in the time domain, active damping with a desired phase lead might be introduced by simple linear filters. The effect of phase lead is therefore illustrated in terms of two filter models of first and second order, respectively. These models are designed to accommodate desired properties in the low- and high-frequency regimes, and around the cut-off frequency, much in the spirit of the design procedures based on Bode plots and frequency representation of compensators, see e.g. Refs. [4,16]. A numerical example is presented to illustrated the findings.

2. Dampers on discrete structures

The equations of motion for the displacements $\mathbf{q}(t)$ of a linear discrete system with negligible structural damping can be written in the following general form:

$$\mathbf{M}\ddot{\mathbf{q}}(t) + \mathbf{K}\mathbf{q}(t) = \mathbf{f}(t), \tag{1}$$

where $\mathbf{M}$ and $\mathbf{K}$ represent the mass and the stiffness matrix. The response is to be characterized by its modal properties and $\mathbf{f}(t)$ therefore represents the effect of the external dampers on the system.

The effect of a single damper on the structure is described in terms of its influence vector $\mathbf{w}$ and the time dependence of the force $f(t)$,

$$\mathbf{f}(t) = -\mathbf{w}f(t). \tag{2}$$

The damper may be connected to a point outside the structure, thereby acting on absolute motion as illustrated in Fig. 1a with $\mathbf{w}^{\mathrm{T}} = [0,\ 0,\ 1,\ 0]$. Or it may connect two points of the structure, thereby acting through their relative motion as illustrated in Fig. 1b with $\mathbf{w}^{\mathrm{T}} = [0,\ -1,\ 1,\ 0]$. The damper is linear and collocated, and the damper force is therefore linear in the local displacement $q_d = \mathbf{w}^{\mathrm{T}}\mathbf{q}$. It is conveniently expressed in the frequency domain in terms of a gain factor g and a transfer function $H(\omega)$,

$$f(\omega) = gH(\omega)q_d(\omega). \tag{3}$$

In the classical case of viscous damping the damper force is proportional to velocity $f(t) = c\dot{q}_d(t)$, whereby the transfer function becomes purely imaginary $H(\omega) = \mathrm{i}\omega$, while the gain corresponds to the damping coefficient $g = c$. The present format considers a general representation, where the transfer function contains both a real and an imaginary part.

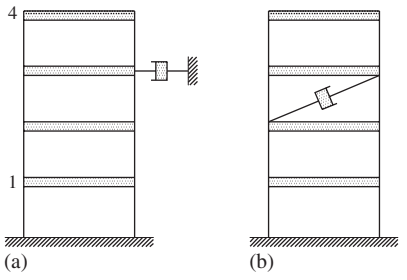

Fig. 1. Damper acting on (a) full motion or (b) relative motion.

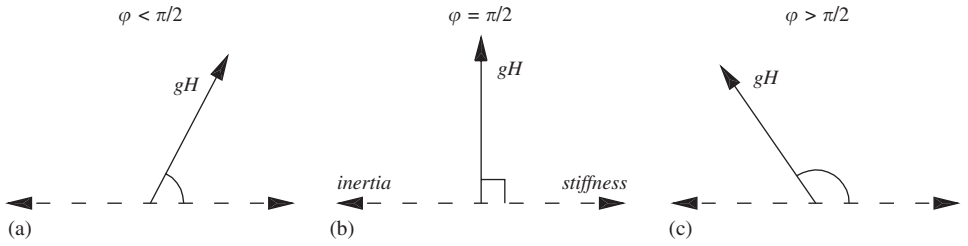

Fig. 2. Force diagram: (a) Passive, (b) viscous and (c) active damper.

Substitution into Eq. (2) leads to the frequency representation of the force vector,

$$\mathbf{f}(\omega) = -gH(\omega)\mathbf{w}\mathbf{w}^{\mathrm{T}}\mathbf{q}(\omega), \tag{4}$$

where $gH(\omega)\mathbf{w}\mathbf{w}^{\mathrm{T}}$ appears as the external damping matrix. Substitution of Eq. (4) into the frequency representation of Eq. (1) leads to the force balance equation,

$$(\mathbf{K} - \omega^2\mathbf{M} + gH(\omega)\mathbf{w}\mathbf{w}^{\mathrm{T}})\mathbf{q}(\omega) = \mathbf{0}. \tag{5}$$

For vanishing gain $g = 0$ the real-valued frequency equations of the undamped system with real-valued natural frequencies ω are recovered. The presence of the damper term in Eq. (5) leads to complex-valued solutions of ω. These are commonly expressed in terms of the damping ratio ζ in the form

$$\omega = |\omega|\left(\sqrt{1-\zeta^2} + \mathrm{i}\zeta\right). \tag{6}$$

While the effect, and thereby the tuning, of the damper is governed by the gain g the frequency characteristics are represented by the transfer function $H(\omega)$, where the real part $\mathrm{Re}[H(\omega)]$ represents the stiffness component, while the imaginary part $\mathrm{Im}[H(\omega)]$ represents viscosity. The transfer function is conveniently formulated in terms of the magnitude $|H|$ and the corresponding phase angle φ,

$$H(\omega) = |H|\exp(\mathrm{i}\varphi). \tag{7}$$

The phase angle is defined as the angle in the complex H-plane relative to the real axis,

$$\tan\varphi = \frac{\mathrm{Im}[H(\omega)]}{\mathrm{Re}[H(\omega)]}, \quad 0 < \varphi < \pi. \tag{8}$$

The characteristics of the damper may be classified in terms of the phase angle, as illustrated by the force diagrams in Fig. 2. Dissipation of energy requires that $g\,\mathrm{Im}[H(\omega)] > 0$, and the phase angle is therefore lying in the interval $0 < \varphi < \pi$. The intermediate case $\varphi = \pi/2$ in Fig. 2b represents viscous damping, where the force is fully in phase with velocity. This idealized case can either be realized by a passive device or by velocity feedback. Fig. 2a shows a damper that lags velocity with a phase angle $\varphi < \pi/2$. This type of damping can also be realized by passive devices—e.g. viscosity with memory effects, or by active or semi-active means, where the damper properties may be varied in time according to some desired control law. The last case in Fig. 2c represents a damper that leads velocity with a phase angle $\varphi > \pi/2$. This damper has a force component in phase with negative stiffness, and therefore requires a fully active device to be realized. A main objective of the present paper is to illustrate the potential increase in damping efficiency that can be obtained by a damper with a phase angle larger than $\pi/2$.

3. Two-component representation

The presence of local dampers leads to complex-valued modal solutions of the force balance equation. Common system reduction techniques rely on a decomposition in terms of the associated complex mode shapes, where the real part represents the actual vibration form, while the imaginary part represents the time delay introduced by the damper. A simplified approach developed by Main and Krenk [11] considers the

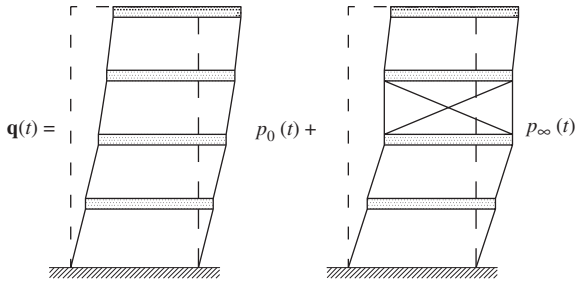

Fig. 3. Decomposition via $\mathbf{u}_0$ and $\mathbf{u}_\infty$.

projection of the full state on to a subspace expanded by the limiting mode shapes for zero gain $\mathbf{u}_0$ and infinite gain $\mathbf{u}_\infty$, respectively. The latter corresponds to the mode shape of the equivalent system where the damper link is fully locked. These mode shapes are real and are easily determined from the numerical model. This two-component representation is exact in the limits for zero and for infinite gain and turns out to be quite accurate over the full gain interval in many cases. The representation can be written as

$$\mathbf{q}(t) = \mathbf{u}_0 p_0(t) + \mathbf{u}_\infty p_\infty(t) = \mathbf{S}\mathbf{p}(t), \tag{9}$$

where the real-valued modal matrix $\mathbf{S} = [\mathbf{u}_0 \ \ \mathbf{u}_\infty]$ spans the reduced subspace, while $\mathbf{p} = [p_0 \ \ p_\infty]^{\mathrm{T}}$ contains the corresponding modal variables. The interpolation between the undamped and infinitely damped mode shapes is illustrated in Fig. 3 for the first mode of the structure shown in Fig. 1b.

The undamped mode shape $\mathbf{u}_0$ is found as the eigenvector of the undamped eigenvalue problem, which follows from Eq. (5) for $g = 0$,

$$(\mathbf{K} - \omega_0^2 \mathbf{M})\mathbf{u}_0 = \mathbf{0}. \tag{10}$$

The mode shape $\mathbf{u}_\infty$ is the eigenvector of the equivalent eigenvalue problem arising when the damper is locked for $g \to \infty$. In the force balance equation (5) clamping of the damper introduces reaction forces represented by the reaction vector $\mathbf{r}$,

$$(\mathbf{K} - \omega_\infty^2 \mathbf{M})\mathbf{u}_\infty = \mathbf{r}. \tag{11}$$

In this equation ω_∞ is the corresponding natural frequency of the structure with a clamped damper link. This eigenvalue problem is solved by first eliminating the degrees of freedom that are non-zero in $\mathbf{r}$, and then solving the resulting homogenous eigenvalue problem. This reduces the number of vibration modes. In the example illustrated in Fig. 3 the number of modes is reduced from 4 to 3. Thus, the use of the representation (9) in terms of a 'matching pair' of mode shapes is limited to modes that retain their identity when clamping the damper.

By construction the mode shape $\mathbf{u}_\infty$ is orthogonal to the influence vector,

$$\mathbf{u}_\infty^{\mathrm{T}} \mathbf{w} = 0. \tag{12}$$

And since $\mathbf{r}$ is proportional to $\mathbf{w}$, an equivalent constraint relation exists for the reaction vector,

$$\mathbf{u}_\infty^{\mathrm{T}} \mathbf{r} = 0. \tag{13}$$

Thus, pre-multiplication of Eq. (11) by $\mathbf{u}_\infty^{\mathrm{T}}$ makes the right-hand side vanish. The infinitely damped system is therefore orthogonal in the same way as the undamped system, and the various mode shapes are normalized as follows:

$$\begin{aligned} \mathbf{u}_0^{\mathrm{T}} \mathbf{M} \mathbf{u}_0 &= 1, \qquad \mathbf{u}_0^{\mathrm{T}} \mathbf{K} \mathbf{u}_0 = \omega_0^2, \\ \mathbf{u}_\infty^{\mathrm{T}} \mathbf{M} \mathbf{u}_\infty &= 1, \qquad \mathbf{u}_\infty^{\mathrm{T}} \mathbf{K} \mathbf{u}_\infty = \omega_\infty^2. \end{aligned} \tag{14}$$

The equations of motion in Eq. (1) satisfy the virtual work equation obtained via pre-multiplication by the virtual displacement field $\delta\mathbf{q}^{\mathrm{T}}$,

$$\delta\mathbf{q}^{\mathrm{T}}(\mathbf{M}\ddot{\mathbf{q}} + \mathbf{K}\mathbf{q} + \mathbf{w}f) = 0. \tag{15}$$

Dynamic equilibrium for the reduced system is obtained via the modal representation in Eq. (9), which also holds for the virtual displacement $\delta\mathbf{q} = \mathbf{S}\delta\mathbf{p}$. Substitution of this representation leads to the isolation of the reduced virtual modal displacement,

$$\delta\mathbf{p}^{\mathrm{T}}(\mathbf{S}^{\mathrm{T}}\mathbf{M}\mathbf{S}\,\ddot{\mathbf{p}} + \mathbf{S}^{\mathrm{T}}\mathbf{K}\mathbf{S}\mathbf{p} + \mathbf{S}^{\mathrm{T}}\mathbf{w}f) = 0, \tag{16}$$

whereby the expression inside the parenthesis must vanish for all values of $\delta\mathbf{p}$. The equation of motion for the reduced system is therefore given as

$$\mathbf{S}^{\mathrm{T}}\mathbf{M}\mathbf{S}\,\ddot{\mathbf{p}} + \mathbf{S}^{\mathrm{T}}\mathbf{K}\mathbf{S}\mathbf{p} = -\mathbf{S}^{\mathrm{T}}\mathbf{w}f. \tag{17}$$

When the matrix multiplications are carried out the reduced equations of motion are found to be

$$\begin{bmatrix} 1 & 1-\gamma \\ 1-\gamma & 1 \end{bmatrix}\begin{bmatrix} \ddot{p}_0 \\ \ddot{p}_\infty \end{bmatrix} + \begin{bmatrix} \omega_0^2 & \omega_0^2(1-\gamma) \\ \omega_0^2(1-\gamma) & \omega_\infty^2 \end{bmatrix}\begin{bmatrix} p_0 \\ p_\infty \end{bmatrix} = -\begin{bmatrix} u_0 \\ 0 \end{bmatrix} f. \tag{18}$$

In this system of equations u_0 is the modal amplitude conjugate to the damper force,

$$u_0 = \mathbf{w}^{\mathrm{T}}\mathbf{u}_0. \tag{19}$$

The modal amplitude u_0 appears as the counterpart to the local damper amplitude q_d defined in connection with Eq. (3) for the full system representation. Due to the constraint condition (12), the effect of the damper solely enters the system via the undamped mode shape $\mathbf{u}_0$, and effective damping therefore requires a non-vanishing value of u_0. This constitutes the controllability condition for collocated damping. The parameter γ represents the coupling between the undamped and the infinitely damped mode shape,

$$\mathbf{u}_\infty^{\mathrm{T}}\mathbf{M}\mathbf{u}_0 = 1 - \tfrac{1}{2}\Delta\mathbf{u}_\infty^{\mathrm{T}}\mathbf{M}\Delta\mathbf{u}_\infty = 1-\gamma, \quad \Delta\mathbf{u}_\infty = \mathbf{u}_\infty - \mathbf{u}_0, \tag{20}$$

where $\Delta\mathbf{u}_\infty$ is the difference in mode shape due to clamping of the damper. For 'small' changes in the mode shape due to clamping the coupling parameter γ is close to zero. As demonstrated by Main and Krenk [11] the approximation $\gamma = 0$ can be used to obtain a simple estimate of the damping effect on mode shapes with moderate changes, while a more detailed and accurate analysis with $\gamma > 0$ can be performed for modes with larger changes.

4. Modal damping

A solution for the natural frequency is obtained by considering the frequency representation of the reduced variables

$$p_0(t) = \mathrm{Re}[\tilde{p}_0\,\exp(\mathrm{i}\omega t)], \quad p_\infty(t) = \mathrm{Re}[\tilde{p}_\infty\exp(\mathrm{i}\omega t)], \tag{21}$$

where complex amplitudes are indicated by a tilde. The corresponding frequency representation of the damper force then follows directly from Eq. (3),

$$f(t) = g u_0\,\mathrm{Re}[H(\omega)\tilde{p}_0\exp(\mathrm{i}\omega t)]. \tag{22}$$

Substitution of the full complex representations of Eqs. (21) and (22) into the reduced set of dynamic equations (18) leads to the following determinant equation:

$$\begin{bmatrix} \omega_0^2 - \omega^2 + g u_0^2 H(\omega) & (1-\gamma)(\omega_0^2-\omega^2) \\ (1-\gamma)(\omega_0^2-\omega^2) & \omega_\infty^2 - \omega^2 \end{bmatrix}\begin{bmatrix} \tilde{p}_0 \\ \tilde{p}_\infty \end{bmatrix} = \begin{bmatrix} 0 \\ 0 \end{bmatrix}, \tag{23}$$

where the effect of the external damper is contained in the term $g u_0^2 H(\omega)$. Non-trivial solutions of Eq. (23) implies a vanishing determinant, leading to the characteristic equation

$$(\omega^2-\omega_0^2)[\omega_\infty^2 - \omega_0^2 - (\omega^2-\omega_0^2)(1-(1-\gamma)^2)] = g u_0^2 H(\omega)(\omega_\infty^2 - \omega^2). \tag{24}$$

Following Main and Krenk [11] the characteristic equation can be rearranged in a format where the transfer function $H(\omega)$ is isolated on the right-hand side of the equation. When change in the quadratic

frequencies are denoted

$$\Delta\omega^2 = \omega^2 - \omega_0^2, \quad \Delta\omega_\infty^2 = \omega_\infty^2 - \omega_0^2, \tag{25}$$

the characteristic equation is rearranged in the form

$$\frac{\Delta\omega^2}{\Delta\omega_\infty^2} \simeq \frac{vH(\omega)}{1 - (\Delta\omega^2/\Delta\omega_\infty^2)(1-(1-\gamma)^2) + vH(\omega)}, \quad v = g\frac{u_0^2}{\Delta\omega_\infty^2}, \tag{26}$$

where v is the non-dimensional gain value. If there are only small changes in the frequency ω due to damping, an approximate solution can be obtained by using a fixed representative value, e.g. ω_0, on the right-hand side. For larger changes of frequency this solution can be improved by fixed point iteration. The efficiency and accuracy of this formula is illustrated at the end of the paper in connection with the numerical example.

A more detailed study of the damping effect calls for an explicit relation between the natural frequency and the effect of the damper. This is obtained by assuming that $\gamma \ll 1$, whereby the middle term of the denominator in Eq. (26) vanishes. This leads to the expression

$$\frac{\Delta\omega^2}{\Delta\omega_\infty^2} \simeq \frac{vH(\omega)}{1 + vH(\omega)}. \tag{27}$$

This parametric representation indicates the behavior of the natural frequency in the complex plane, schematically illustrated in Fig. 4. It follows that Eq. (27) recovers the solutions for zero gain ω_0^2 and for infinite gain ω_∞^2. For finite values of the gain the natural frequency follows a particular locus in the complex plane. The shape of this locus depends on the properties of the damper represented by the transfer function $H(\omega)$.

Modal damping can be represented by the imaginary part of the natural frequency, representing energy dissipation per unit time. However, for stationary resonant response the magnitude of the response is inversely proportional to the damping ratio ζ, introduced in Eq. (6) as the relative imaginary part of the natural frequency,

$$\zeta = \frac{\mathrm{Im}[\omega]}{|\omega|}. \tag{28}$$

Since response of flexible structures is often governed by resonance, tuning on the basis of damping ratio is adopted in the following. There is an interesting analogy to tuned mass dampers, for which it has recently been demonstrated that classical frequency tuning leads to equal damping ratio of the two coupled modes [17].

The present analysis is based on the square of the natural frequency. The relation between the relative imaginary part of ω and ω^2, respectively, is given as

$$\frac{\mathrm{Im}[\omega^2]}{|\omega^2|} = 2\frac{\mathrm{Im}[\omega]}{|\omega|}\frac{\mathrm{Re}[\omega]}{|\omega|}. \tag{29}$$

For moderate damping $\mathrm{Re}[\omega]/|\omega| \simeq 1$, and the damping ratio can be estimated directly from ω^2. Substitution of Eq. (29) into Eq. (28) then gives

$$\zeta \simeq \frac{1}{2}\frac{\mathrm{Im}[\omega^2]}{|\omega^2|} \simeq \frac{\mathrm{Im}[\Delta\omega^2]}{\omega_0^2 + \omega_\infty^2}, \tag{30}$$

where the last relation is obtained by introducing $\mathrm{Im}[\omega^2] = \mathrm{Im}[\omega_0^2 + \Delta\omega^2] = \mathrm{Im}[\Delta\omega^2]$ and by the approximation $|\omega^2| = |\omega_0^2 + \Delta\omega^2| \simeq \frac{1}{2}(\omega_0^2 + \omega_\infty^2)$. The damping ratio thus appears as half the angle in the ω^2-plane relative to the real axis.

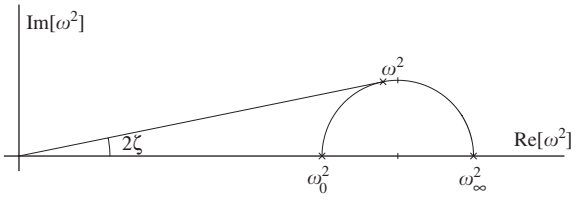

Fig. 4. Complex locus of ω^2.

Substitution of Eq. (27) into Eq. (30) followed by a representation of the transfer function in terms of its real and imaginary part leads to the following expression for the damping ratio,

$$\zeta \simeq \frac{\Delta\omega_\infty^2}{\omega_0^2+\omega_\infty^2}\,\frac{v\,\mathrm{Im}[H(\omega)]}{(1+v\,\mathrm{Re}[H(\omega)])^2+(v\,\mathrm{Im}[H(\omega)])^2}. \tag{31}$$

For small gain values the terms that are quadratic in v can be omitted, and the asymptotic expression for the damping ratio is then given as

$$\zeta \simeq \frac{\Delta\omega_\infty^2}{\omega_0^2+\omega_\infty^2}\,\frac{v\,\mathrm{Im}[H(\omega)]}{1+2v\,\mathrm{Re}[H(\omega)]} \quad \text{for } v\ll 1. \tag{32}$$

In the limit of vanishing gain the damping ratio is hereby proportional to the imaginary part of the transfer function. For finite values of the gain the presence of the real part in the denominator becomes significant, and attainable damping is seen to increase with decreasing stiffness. In particular the situation where $v\,\mathrm{Re}[H]<0$ leads to large damping effects. This situation corresponds to a damper with negative stiffness. The effect of negative stiffness is illustrated in the following section by ideal energy dissipation through a simple radiation condition.

5. Ideal damping of one-dimensional structures

The objective of damping is to dissipate energy, and a good damping device should permit sufficient structural motion to lead the energy to the damper and to provide the necessary dissipation in the damper. The combination of these requirements can be illustrated by a simple one-dimensional example. The equation of motion for continuous structural elements can typically be written in the following general form

$$\mathscr{D}_x u(x,t)-\rho\ddot{u}(x,t)=f(t)\delta(x-a), \tag{33}$$

where $u(x,t)$ represents the displacement, $\mathscr{D}_x$ denotes the spatial differential operator, and time differentiation is denoted by a dot over the symbol. The control force $f(t)$ is a collocated damper acting at the location $x=a$.

The basic requirements to the damper are conveniently illustrated by the simple case where the operator represents the second-order spatial derivative. This system might be thought of as a simply supported string with a damper attached at a distance a from the left support, as illustrated in Fig. 5a. When the damper is located close to one of the supports, efficiency implies absorption of the energy approaching from the string without any reflection. This requires a tuning of the damper in terms of the simple one-dimensional wave equation,

$$u''(x,t)-s^{-2}\ddot{u}(x,t)=0, \quad s=\sqrt{T/\rho}, \tag{34}$$

where s is the wave speed and spatial derivatives are denoted by a prime. Expressions for the two waveforms moving to the left and right, respectively, are obtained by effectively factorizing the wave equation,

$$[u'(x,t)-s^{-1}\dot{u}(x,t)][u'(x,t)+s^{-1}\dot{u}(x,t)]=0. \tag{35}$$

In this case, where the damper is located close to the left support, optimal damping requires radiation of the corresponding left waveform, whereby the first factor in Eq. (35) must vanish at the location of the damper. This implies that the transverse force component just to the right of the damper is $Tu'_a(t)=T\dot{u}_a(t)/s$, corresponding to an equivalent problem in which the combined effect of the left support and the force $f(t)$ is replaced by an impedance condition, represented by a viscous damper with parameter $c=\sqrt{T\rho}$, as illustrated in Fig. 5b. Thus, the solution to this problem appears as ideal boundary control of the wave equation.

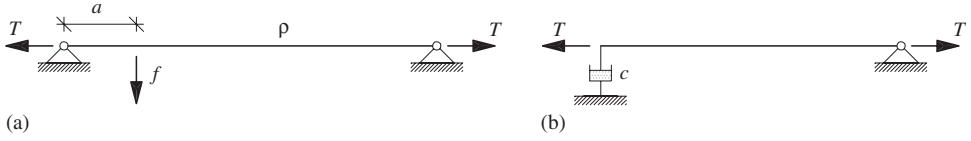

Fig. 5. (a) String with external damper and (b) radiation by impedance condition.

In the actual problem in Fig. 5a the left support provides an additional transverse force component. When the damper is assumed to be located sufficiently close to the support the magnitude of this force is approximately $(T/a)u_a(t)$. This force should be compensated by $f(t)$ and the resulting optimal control force is then given as

$$f(t) = T[\dot{u}_a(t)/s - u_a(t)/a]. \tag{36}$$

The radiation condition can thus be realized by a combination of an impedance term, $\sqrt{T\rho}\,\dot{u}_a$, and a negative stiffness term, $-(T/a)u_a$. In the frequency domain the linear control force (36) is characterized by the transfer function

$$H(\omega) = \mathrm{i}\omega\sqrt{\rho a/T} - 1, \quad g = T/a. \tag{37}$$

This transfer function represents a proportional- and derivative-type controller, where the imaginary part introduces optimal energy dissipation through the derivative term in phase with velocity, $\sqrt{\rho a/T}$, while the proportional term represents the negative stiffness component, here normalized to unity. Ideal energy dissipation in terms of the wave equation leads to the introduction of a significant negative real part of the transfer function. This negative stiffness component, $g\,\mathrm{Re}[H] = -T/a$, eliminates all structural stiffness at the location of the damper, whereby additional negative stiffness would destabilize the system. Thus, optimal damping occurs at the limit of stability.

The combined effect of viscosity and negative stiffness in Eq. (37) is represented by the phase angle

$$\tan\varphi = -\pi\frac{a}{l}\frac{\omega}{\omega_1^0}, \quad \omega_1^0 = \frac{\pi}{l}\sqrt{T/\rho}, \tag{38}$$

where ω_1^0 denotes the undamped natural frequency of the first mode with l being the length of the string. For a damper location close to the support, $a/l \ll 1$, the phase angle will be close to π. Damping by the radiation condition is therefore equivalent to damping with a significant phase lead.

An alternative approach to damping of an incoming wave in beams and bars has been considered in Refs. [18,19]. The principle consists of an equal splitting of the reflected and transmitted wave. Both of these waves get half of the amplitude of the incident wave, and in total they therefore carry half the energy, while the other half is dissipated by the damper. The efficiency of this principle relies on the absence of a boundary condition reflecting the wave. The present approach is fundamentally different since the damper is located sufficiently close to the support to secure that waves only approach from one side, whereby an impedance condition can be applied. In the ideal case this leads to full absorption of energy. A similar approach was used in Ref. [20] for damping and base isolation of a discrete shear frame structure subjected to ground excitation. Although energy radiation conditions are very effective, they are difficult to formulate and to realize for more general types of structures with arbitrary damper locations. In a general sense, the introduction of negative stiffness might help to increase the damper stroke and thereby attract additional energy towards the location of the damper. This simple property of negative stiffness—or phase lead—may therefore be carried on as a desirable property of active dampers. An effective way of implementing phase lead is suggested in the following section in terms of simple linear filters with desirable low-pass properties.

6. Damper models with phase lead

The objectives of the damper models in this section are to apply large damping in the low-frequency range, while attenuating undesirable noisy components of the structure in the high-frequency range. This means that the filters should exhibit low-pass behavior with a phase lead below the cut-off frequency.

6.1. First-order filter

A simple damper model with phase lead follows from the general first-order filter

$$f(t) + \tau_f\dot{f}(t) = g_0[q_d(t) + \tau_u\dot{q}_d(t)] \tag{39}$$

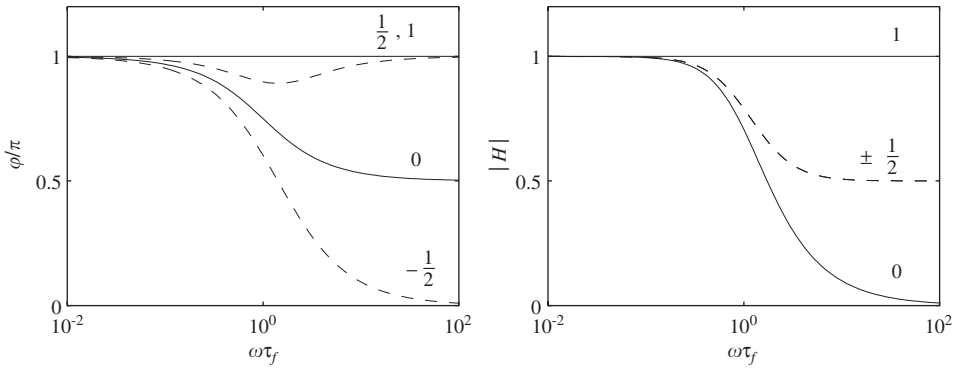

Fig. 6. Phase angle and magnitude. Lag compensator: $g_\infty/g_0 = -\frac{1}{2}$, 0, $\frac{1}{2}$ and 1.

with gain g_0 and time scales τ_u and τ_f. The cut-off frequency of this filter is $1/\tau_f$. The characteristics of this filter are easily identified by re-arranging it into the so-called relaxation format, where the terms are collected by their order of differentiation,

$$[f(t) - g_0 q_d(t)] + \tau_f[\dot{f}(t) - g_\infty \dot{q}_d(t)] = 0. \tag{40}$$

This format clearly identifies g_0 and $g_\infty = (\tau_u/\tau_f)g_0$ as the low- and high-frequency stiffness, respectively. It turns out that, for the phase angle to approach π in the low-frequency limit, the filter should have a stiffness ratio $g_\infty/g_0 \leqslant 1$. This means that a phase lead follows from a filter of lag compensator type. The phase angle and magnitude of this filter are presented in Fig. 6 for various values of g_∞/g_0. It follows directly from the relaxation format (40) that a vanishing high-frequency magnitude implies that $g_\infty = 0$. Fig. 6 shows that this case corresponds to a phase angle of $\pi/2$ in the high-frequency range. This filter hereby satisfies the requirements of low-frequency phase lead and a vanishing high-frequency magnitude, and the governing equation for the resulting filter is therefore given as

$$f(t) + \tau_f \dot{f}(t) = g_0 q_d(t). \tag{41}$$

The corresponding expression for phase angle and magnitude are easily derived as

$$\tan\varphi = -\omega\tau_f, \quad |H| = \sqrt{\frac{1}{1 + (\omega\tau_f)^2}}. \tag{42}$$

In a design situation the time scale τ_f is typically chosen so that the modes of interest are located well below the cut-off frequency, while the tuning of the damper relies on the gain g_0. Dissipation of energy requires that $g_0 \,\mathrm{Im}[H(\omega)] > 0$. For the filter in Eq. (41) this means that $g_0 < 0$, and this yields a phase lead, and thereby a negative stiffness, over the entire frequency range, as illustrated in Fig. 6.

6.2. Second-order filter

Additional flexibility is effectively introduced by a filter of second order. In a general format the acceleration feedback is introduced with a minus to secure a dissipative damper force. This leads to a filter of the form

$$\ddot{f}(t) + 2\zeta_f\omega_f\dot{f}(t) + \omega_f^2 f(t) = g_\infty[-\ddot{q}_d(t) + 2\zeta_u\omega_u\dot{q}_d(t) + \omega_u^2 q_d(t)]. \tag{43}$$

For the special case where $\zeta_u = 0$ this general format recovers well-known filter models from the literature. For $\omega_u \to \infty$ it recovers 'positive position feedback', [8], while for $\omega_u = 0$ it leads to simple 'acceleration feedback', [9]. The present approach can therefore be considered as an interpolation between these limiting models via the finite damping ratio ζ_u.

The relaxation format of Eq. (43) appears as

$$[\ddot{f}(t) + g_\infty\ddot{q}_d(t)] + 2\omega_f[\zeta_f\dot{f}(t) - g_\infty\zeta_u\beta\dot{q}_d(t)] + \omega_f^2[f(t) - g_\infty\beta^2 q_d(t)] = 0, \tag{44}$$

where $\beta = \omega_u/\omega_f$ represents the frequency ratio. $-g_\infty$ represents the high-frequency stiffness, while the equivalent low-frequency stiffness is given as $g_0 = \beta^2 g_\infty$. Thus, for the high-frequency magnitude to vanish the corresponding high-frequency stiffness should vanish as well, i.e. $g_\infty \to 0$. However, this limit should be approached in a manner that leads to the desired behavior in the low-frequency range and around the cut-off frequency. This introduces certain restrictions on ζ_u. First of all, dissipation of energy requires that $g_\infty \operatorname{Im}[H(\omega)] > 0$. For the filter equation in Eq. (43) this means that $g_\infty < 0$ and that the damping ratio ζ_u satisfies the inequality

$$-1 \leqslant \beta \frac{\zeta_u}{\zeta_f} \leqslant \beta^2. \tag{45}$$

A parametric representation of ζ_u by the mean value of the two limits in Eq. (45) secures a dissipative force component of the damper,

$$\zeta_u = \tfrac{1}{2}(\beta - 1/\beta)\zeta_f. \tag{46}$$

Substitution of this parametric representation leads to an effective separation of the right-hand side of Eq. (43) in terms of low- and high-frequency stiffness,

$$\ddot{f}(t) + 2\zeta_f\omega_f\dot{f}(t) + \omega_f^2 f(t) = g_0[\zeta_f\omega_f\dot{q}_d(t) + \omega_f^2 q_d(t)] - g_\infty[\ddot{q}_d(t) + \zeta_f\omega_f\dot{q}_d(t)] \tag{47}$$

and the final equation for the second-order filter then follows by $g_\infty = 0$,

$$\ddot{f}(t) + 2\zeta_f\omega_f\dot{f}(t) + \omega_f^2 f(t) = g_0[\zeta_f\omega_f\dot{q}_d(t) + \omega_f^2 q_d(t)], \tag{48}$$

where $g_0 < 0$. The damping ratio ζ_f controls the roll-off properties around the cut-off frequency ω_f of the filter. A suitable damping ratio can be found by considering the phase angle given as

$$\tan\varphi = -\zeta_f r \frac{1 + r^2}{1 - (1 - 2\zeta_f^2)r^2}. \tag{49}$$

Fig. 7 presents the phase angle and magnitude for various values of the damping ratio: $\zeta_f = 0.5$, $1/\sqrt{2}$ and 1. When $\zeta_f = 1$ the second-order filter recovers the first-order filter given in Eq. (41). While the roll-off properties of phase angle and magnitude improve with decreasing ζ_f, the phase angle exhibits an 'undershoot' around cut-off for damping ratios $\zeta_f < 1/\sqrt{2}$, as illustrated for $\zeta_f = 0.5$ in Fig. 7a. A compromise between large roll-off and minimum undershoot is obtained by $\zeta_f = 1/\sqrt{2}$, which is represented by solid lines in Fig. 7.

The damping efficiency of both filter models relies on the phase lead in the low-frequency range. This phase lead is realized by a negative stiffness component, and the gain values of the filters are therefore bounded by stability. The limit of stability is addressed next.

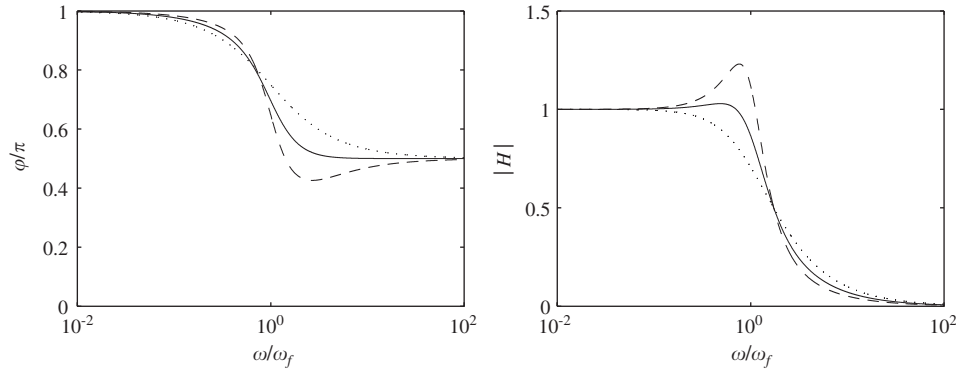

Fig. 7. Frequency properties: $\zeta_f = 0.5$ (– – –), $1/\sqrt{2}$ (——) and 1 (· · · · · ·).

6.3. Stability limit

Stability of dynamic systems is conveniently analyzed by investigating the stability of the individual modes. The equation of motion for a single mode is found by introducing the modal representation $\mathbf{q}(t) = \mathbf{u}_0 p_0(t)$ into Eqs. (1) and (2), and then pre-multiplying the combined equation with $\mathbf{u}_0^{\mathrm{T}}$,

$$\ddot{p}_0(t) + \omega_0^2 p_0(t) = -u_0 f(t). \tag{50}$$

The corresponding modal representation of the equation for the general first-order filter in Eq. (39) is given as

$$f(t) + \tau_f \dot{f}(t) = g_0 u_0 [p_0(t) + \tau_u \dot{p}_0(t)]. \tag{51}$$

Stability of the combined system, Eqs. (50) and (51), depends on the properties of the eigenvalue λ, introduced by assuming solutions of exponential form,

$$p_0(t) = \tilde{p}_0 \exp(\lambda t), \quad f(t) = \tilde{f} \exp(\lambda t), \tag{52}$$

where the associated amplitudes are represented by a tilde. Substitution of these solutions into Eqs. (50) and (51), followed by elimination of $\tilde{f}$, leads to the characteristic equation

$$\tau_f \lambda [\lambda^2 + \omega_0^2 + g_\infty u_0^2] + [\lambda^2 + \omega_0^2 + g_0 u_0^2] = 0. \tag{53}$$

Stability requires that the real part of the roots of this polynomial are non-positive, i.e. $\mathrm{Re}[\lambda] \leqslant 0$ for all λ. This condition can readily be checked by the Routh–Hurwitz criterium, see e.g. [2]. Since $g_0 \leqslant g_\infty$ the constant term in Eq. (53) represents the most restrictive part, and stability is therefore secured as long as the constant term is non-negative. This leads to the stability condition

$$\omega_0^2 + g_0 u_0^2 \geqslant 0. \tag{54}$$

Hence, stability of the full system requires that this inequality is satisfied for all modes. The stiffness of the filter models increases with frequency, and the 'largest' negative stiffness component therefore occurs for zero frequency. This confirms that stability of the system is governed by the constant term of the characteristic equation.

An equivalent approach can be used for the second-order filter, and for reasons of simplicity the analysis is based on the reduced filter equation in Eq. (48), without contribution from acceleration feedback. The modal representation of this filter equation appears as

$$\ddot{f}(t) + 2\zeta_f \omega_f \dot{f}(t) + \omega_f^2 f(t) = g_0 u_0 [\zeta_f \omega_f \dot{p}_0(t) + \omega_f^2 p_0(t)] \tag{55}$$

and the characteristic equation again follows from substituting Eq. (52) into Eqs. (50) and (55), and then eliminating $\tilde{f}$ between these equations.

$$\lambda^4 + 2\zeta_f \omega_f \lambda^3 + (\omega_f^2 + \omega_0^2)\lambda^2 + \zeta_f \omega_f (2\omega_0^2 + g_0 u_0^2)\lambda + \omega_f^2(\omega_0^2 + g_0 u_0^2) = 0. \tag{56}$$

When applying the Routh–Hurwitz criterium to this equation it turns out that it is once again the constant term that is the most critical. This simply means that stability of the second-order filter is secured as long as g_0 satisfies the stability condition in Eq. (54). It should be noted that this condition is identical to the stability limit obtained for positive position feedback in Ref. [21].

The stability condition in Eq. (54) can be re-interpreted in terms of the full system representation, where it states that the effective stiffness matrix $\mathbf{K} + g_0 \mathbf{w}\mathbf{w}^{\mathrm{T}}$ must be at least positive semi-definite, i.e.

$$\det(\mathbf{K} + g_0 \mathbf{w}\mathbf{w}^{\mathrm{T}}) \geqslant 0. \tag{57}$$

The equality, where the effective stiffness matrix becomes singular, corresponds to the situation where the negative stiffness introduced by the damper eliminates all structural stiffness across the damper link. In many situations the limit of stability can be predicted directly from this condition. This is, for instance, the case for the simple shear frame model used in the following numerical example.

7. Damping of shear frame

The objective of this numerical example is to demonstrate the increase in damping efficiency that can be obtained by an active damper with phase lead. Furthermore, the accuracy of the closed form solutions for the natural frequency is discussed by comparison with the exact solution.

7.1. Discrete structure

The example considers a shear frame structure as in Fig. 8, where the damper is attached between two adjacent storeys. The shear frame has n storeys with identical mass m and inter-storey stiffness k. Structural damping is neglected. The equation of motion for the shear frame is expressed by a diagonal mass matrix and a tri-diagonal stiffness matrix,

$$\mathbf{M} = m\begin{bmatrix} 1 & & & \\ & 1 & & \\ & & \ddots & \\ & & & 1 \end{bmatrix}, \quad \mathbf{K} = k\begin{bmatrix} 2 & -1 & & \\ -1 & 2 & & \\ & & \ddots & -1 \\ & & -1 & 1 \end{bmatrix}. \tag{58}$$

This finite difference format of the system equations leads to the following analytical solution for the undamped natural frequencies, see e.g. Ref. [10]:

$$\omega_r^0 = 2\Omega \sin\left(\frac{\pi}{2}\frac{2r-1}{2n+1}\right), \quad r = 1 \ldots n, \tag{59}$$

where r denotes the mode number and where $2\Omega = 2\sqrt{k/m}$ represents the natural frequency of a single element and thereby constitutes an upper limit for the frequencies of the discrete system. In the present example $n = 10$, as illustrated in Fig. 8, and $\Omega = 10\,\text{rad/s}$.

7.2. Location of damper

According to the approximate expression for the damping ratio (31), attainable damping increases with the factor $\Delta\omega_\infty^2/(\omega_\infty^2 + \omega_0^2)$. This means that a proper damper location relies on an adequate difference between the undamped natural frequency and the frequency obtained by locking the damper. The present example considers the two damper locations shown in Fig. 8, where the damper in case 1 operates on the first storey, while in case 2 it acts between the fifth and sixth storey. The influence vectors for these two cases are

$$\mathbf{w}_1^{\mathrm{T}} = [1,\ 0 \ldots 0], \quad \mathbf{w}_2^{\mathrm{T}} = [0,\ 0,\ 0,\ 0,\ -1,\ 1 \ldots 0]. \tag{60}$$

The corresponding parameter for attainable damping is given in Table 1 for modes 1–4. It turns out that, if the damper can only operate between two adjacent storeys, placing the damper between ground and first storey (case 1) is optimal. It is also seen from the table that the expected damping for case 2 is significantly smaller

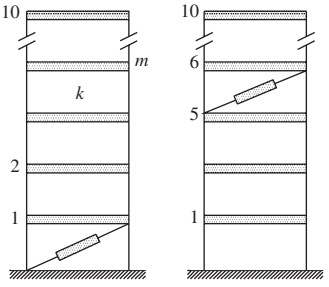

Fig. 8. Ten-storey shear frame. Damper located between: ground and first storey (case 1), fifth and sixth storey (case 2).

Table 1
Attainable damping parameter

	Case	Modes			
		1	2	3	4
$\Delta\omega_\infty^2/(\omega_\infty^2+\omega_0^2)$	1	0.100	0.098	0.095	0.090
	2	0.045	0.059	0.029	0.067

than for case 1. This is in particular the situation for mode 3, where the controllability in case 2 is quite small. In general it is therefore very important to place the damper where the modal displacement over the damper is adequate for the modes of interest.

7.3. Damper properties

Three damper models are considered: the viscous damper, the first-order filter in Eq. (41), and the second-order filter in Eq. (48) with $\zeta_f = 1/\sqrt{2}$.

For flexible structures it is usually the lowest modes, below a certain frequency, that are prone to dynamic excitations, e.g. from wind, wave, or traffic loading. The main objective of the external damper is therefore to apply a sufficient degree of damping to a given number of the lowest modes. In this example the viscous damper is therefore tuned optimally with respect to mode 1. The corresponding optimal gain can be found by the parametric representation in Eq. (27), where maximum damping occurs for $v|H(\omega)| = 1$. For a viscous damper, where $H \simeq \mathrm{i}\omega_0$, this means that the optimal damper coefficient is $c_{\mathrm{opt}} \simeq \Delta\omega_\infty^2/(\omega_0 u_0^2)$.

The performance of the filter models depends on the choice of cut-off frequency, and for mode 1 to be sufficiently damped the cut-off frequency is chosen as the undamped natural frequency of mode 3,

$$1/\tau_f = \omega_f = \omega_3^0.$$

Hereby, both modes 1 and 2 are located below the cut-off frequency. Phase angle and magnitude of the filter models are illustrated in Fig. 9 where the circles ($\circ$) represent the values for the undamped natural frequencies of modes 1–4. It is seen that for modes 1 and 2 the phase angles for the two filter models more or less coincide, while they for the subsequent modes are marginally larger for the first-order filter. Since the magnitude of the second-order filter is larger in the frequency range of interest, it is expected that this model leads to better efficiency for modes 1 and 2.

The limit of stability corresponds to the situation where the negative stiffness of the damper eliminates the structural stiffness across the damper link. For both damper locations the inter-storey stiffness is k, and stability therefore requires that

$$-k \leqslant g_0 \leqslant 0.$$

It is verified by the stability condition in Eq. (57) that the lower limit is in fact the actual limit of stability of the systems.

7.4. Exact natural frequencies

Modal damping is conveniently represented by the damping ratio as the relative imaginary part of the natural frequency. When formulating the dynamic equations in state–space, the exact natural frequency ω_r of mode r is found by solving the generalized eigenvalue problem

$$(\mathbf{A} - \mathrm{i}\omega_r \mathbf{B})\mathbf{u}_r = \mathbf{0}, \tag{61}$$

where $\mathbf{u}_r$ is the corresponding mode shape, and where $\mathbf{A}$ and $\mathbf{B}$ are the representative system matrices.

The system matrices for the three types of dampers are briefly presented below for the sake of completeness. For viscous damping the equations of motion can be written in symmetric form with the state vector

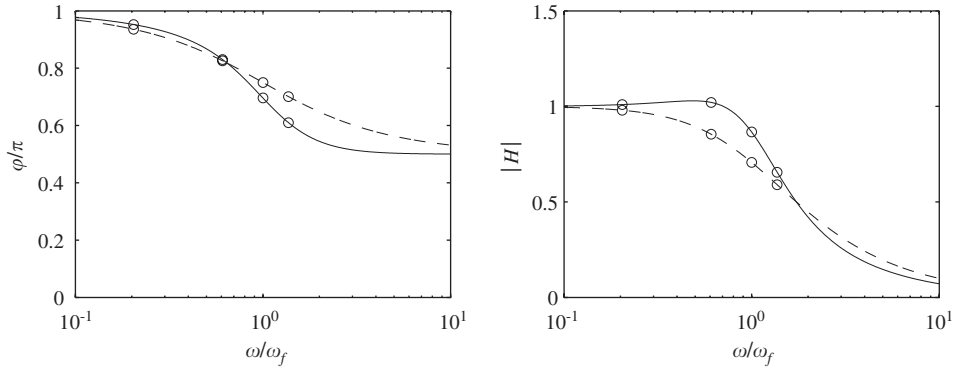

Fig. 9. Frequency properties for first-order filter (– – –) and second-order filter (——). Location of undamped modes 1–4 indicated by (○).

containing displacement and velocity: $\mathbf{z} = [\mathbf{q};\ \dot{\mathbf{q}}]$,

$$\mathbf{A} = \begin{bmatrix} -\mathbf{K} & \mathbf{0} \\ \mathbf{0} & \mathbf{M} \end{bmatrix}, \quad \mathbf{B} = \begin{bmatrix} c\mathbf{w}\mathbf{w}^{\mathrm{T}} & \mathbf{M} \\ \mathbf{M} & \mathbf{0} \end{bmatrix}. \tag{62}$$

For the first-order filter the state vector is augmented by the damper force: $\mathbf{z} = [\mathbf{q};\ \dot{\mathbf{q}};\ f]$. For $g_\infty = 0$ the system matrices also appear on symmetric form,

$$\mathbf{A} = \begin{bmatrix} -\mathbf{K} & \mathbf{0} & -\mathbf{w} \\ \mathbf{0} & \mathbf{M} & \mathbf{0} \\ -\mathbf{w}^{\mathrm{T}} & \mathbf{0} & 1/g_0 \end{bmatrix}, \quad \mathbf{B} = \begin{bmatrix} \mathbf{0} & \mathbf{M} & \mathbf{0} \\ \mathbf{M} & \mathbf{0} & \mathbf{0} \\ \mathbf{0} & \mathbf{0} & -\tau_f/g_0 \end{bmatrix}. \tag{63}$$

For the second-order filter the derivative of the damper force is furthermore included: $\mathbf{z} = [\mathbf{q};\ \dot{\mathbf{q}};\ f;\ \dot{f}]$, and this representation of the state vector leads to a non-symmetric form of $\mathbf{A}$,

$$\mathbf{A} = \begin{bmatrix} -\mathbf{K} & \mathbf{0} & -\mathbf{w} & \mathbf{0} \\ \mathbf{0} & \mathbf{M} & \mathbf{0} & \mathbf{0} \\ g_0\omega_f^2\mathbf{w}^{\mathrm{T}} & g_0\zeta_f\omega_f\mathbf{w}^{\mathrm{T}} & -\omega_f^2 & 0 \\ \mathbf{0} & \mathbf{0} & 0 & 1 \end{bmatrix}, \quad \mathbf{B} = \begin{bmatrix} \mathbf{0} & \mathbf{M} & \mathbf{0} & \mathbf{0} \\ \mathbf{M} & \mathbf{0} & \mathbf{0} & \mathbf{0} \\ \mathbf{0} & \mathbf{0} & 2\zeta_f\omega_f & 1 \\ \mathbf{0} & \mathbf{0} & 1 & 0 \end{bmatrix}. \tag{64}$$

The natural frequencies of modes 1–4 are presented in Fig. 10. The figures show the frequency loci, where the natural frequencies are plotted in the complex plane for increasing gain. The top four figures represent case 1, while the bottom four represent case 2. The various exact natural frequencies are represented by: asterisks (∗) for the viscous damper, crosses (×) for the first-order filter, and plus signs (+) for the second-order filter. For the filter models the natural frequencies are shown for equally spaced gain values, with increments: $\Delta g_0 = -0.01k$, $-0.02k$, $-0.05k$ and $-0.1k$ for modes 1–4, respectively. These increments are mainly chosen for graphical reasons. Table 2 gives the damping ratios for case 1 for particular gain values: $g_0 = -0.5k$, $-0.75k$ and $-k$, where the latter corresponds to the limit of stability. Note that for viscous damping the exact natural frequencies in Fig. 10, and the damping ratios in Table 2, are only given for the optimal gain with respect to mode 1. The entire frequency loci for viscous damping, based on the approximate solution (27), are given by the solid lines in the figure.

7.5. Damping efficiency

It is seen from Fig. 10 that the filter models produce frequency loci with a larger imaginary part, and thereby with larger modal damping, than for viscous damping. The largest damping effect is obtained for modes 1 and 2. They are located below the cut-off frequency of the filters and are therefore subject to a significant phase

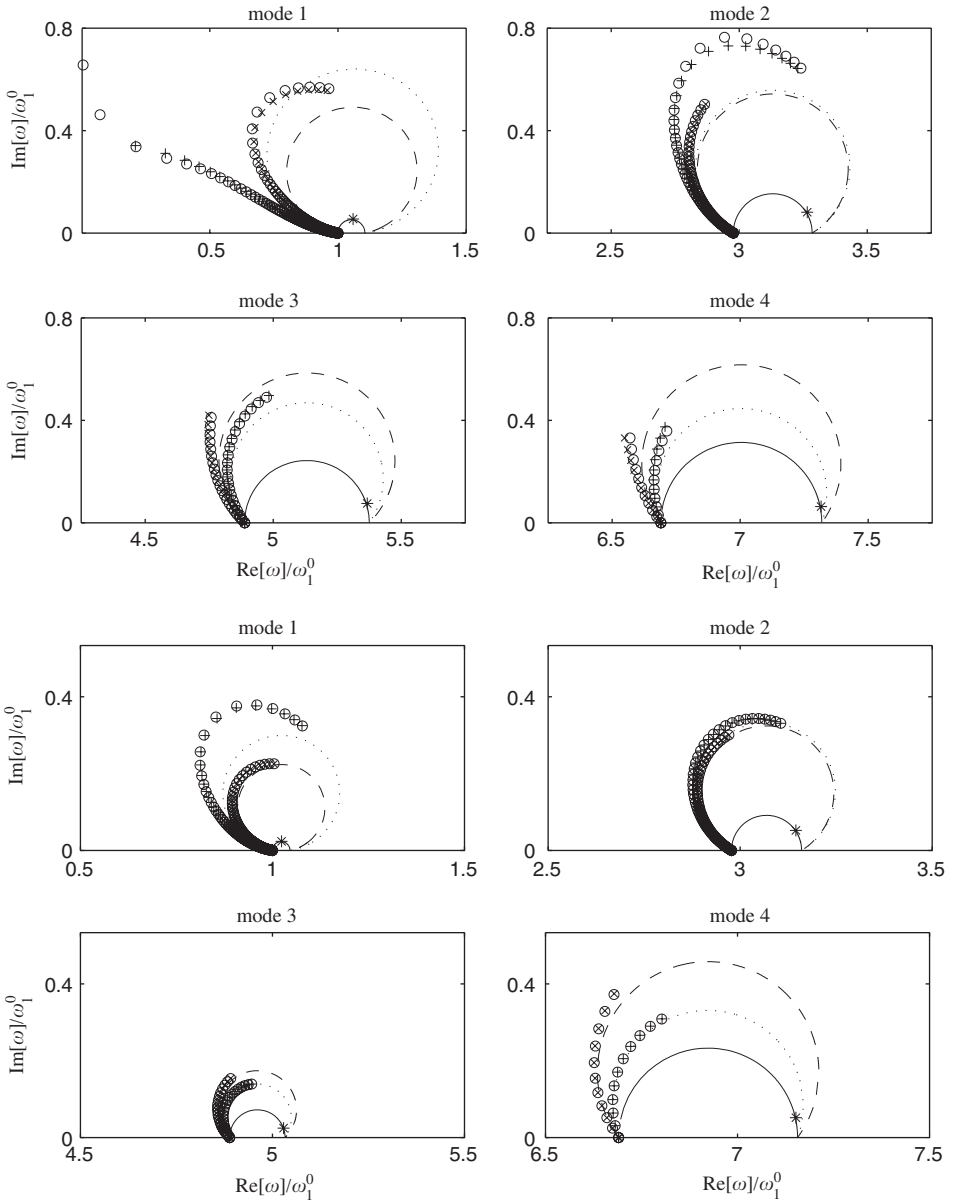

Fig. 10. Frequency locus of modes 1–4. Top four figures: case 1, bottom four: case 2. Viscous damper (——, ∗), first-order filter (– – –, ×, ○) and second-order filter (· · · · · ·, +, ○).

Table 2
Case 1. Damping ratios in for modes 1–4

	Mode 1			Mode 2			Mode 3			Mode 4		
Gain $[-k]$	0.5	0.75	1.0	0.5	0.75	1.0	0.5	0.75	1.0	0.5	0.75	1.0
First order	2.9	11.2	50.3	4.1	9.2	17.3	3.0	6.0	8.8	2.1	3.7	5.1
Second order	2.3	9.1	100	5.5	15.3	19.5	4.3	7.5	9.9	2.5	4.0	5.6
Viscous		5.2			2.5			1.4			0.9	

Viscous optimal for mode 1.

lead and a magnitude close to unity. The damping ratios in Table 2 for these modes are up to 10 times larger compared to viscous damping. The large damping effect of the filter models becomes very evident for case 1, where the second-order filter leads to critically damping of mode 1 for gain values close to the limit of stability, $g_0 \simeq -k$. This type of control corresponds to the idealized situation of base isolation, where the negative stiffness produced by the damper almost completely eliminates the structural stiffness between the ground and first storey. This clearly indicates that the increase in damping obtained by active control with phase lead may become very significant.

As indicated by the parameters in Table 1 the damping efficiency obtained by placing the damper between ground and first storey (case 1) is much larger compared to when it is placed between storeys 5 and 6 (case 2). The decrease in damping due to the reduction in controllability for mode 3 (case 2) is evident from Fig. 10, where the corresponding frequency loci are smaller compared to the other modes.

The damping ratios presented in Table 2 unfortunately indicate that a substantial part of the damping effect is only obtainable for gain values close to the limit of stability. This means that even a small reduction in gain might lead to a severe reduction in damping efficiency. In Table 2 this is clearly illustrated for mode 1, where a decrease in gain from $g_0 = -k$ to $-0.75k$ leads to reduction in damping ratio by around 78% for the first-order filter and even 91% for the second-order filter. Although these are significant reductions, it should be noted that the filter models with $g_0 \simeq -0.75k$ still provide damping ratios that are larger compared to corresponding values for viscous damping.

While damping is very large for the low-frequency modes, the decrease in phase angle and magnitude with frequency leads to an equivalent reduction in efficiency for modes 3 and 4. In this frequency range a viscous damper, specifically tuned to one of these modes, would in fact produce damping that is comparable to that produced by the filter models. However, due to the present tuning with respect to mode 1, the viscous damper appears too stiff for the subsequent modes, and the filter models are therefore still superior.

The difference in damping efficiency between the first- and second-order filters is marginal. However, for modes 1 and 2 it seems as if the second-order filter is slightly better. This is mainly because of the improved magnitude of the second-order filter in the low-frequency range. For modes 3 and 4 the performance of the two filter models is roughly the same, and it seems as if the larger phase lead of the first-order filter cancels the effect from the larger magnitude of the second-order filter.

In general, this example indicates that a large increase in damping, relative to optimal passive means, can be generated by combining a significant phase lead with a magnitude close to unity. It should in particular be noted that the second-order filter is very efficient in the low-frequency range, and provides an effective roll-off around the cut-off frequency.

7.6. Accuracy of approximate solutions

The approximate two-component representation given in Eq. (9) leads to very simple expressions for the natural frequency. The full solution in Eq. (26) is implicit but is easily solved numerically. When coupling effects are neglected this leads to Eq. (27), which appears on explicit form when ω is replaced by ω_0 on the right-hand side.

The implicit equation (26) is presented in a format that is effectively solved by simple fixed point iteration. When tracing the frequency locus with suitable gain increments it is found that no more than 5 iterations for each increment are actually needed to obtained a sufficient accuracy.

The natural frequencies obtained for the filter models from the iterative procedure are illustrated by the circles ($\circ$) in Fig. 10. They are determined for the same gain values as for the exact solutions. It was demonstrated by Main and Krenk [11] that the implicit solution (26) was very accurate for viscous damping. The present example shows that this is also the situation for very aggressive damping with a large phase lead, as for the lower modes in Fig. 10 and in particular for the base isolation of mode 1. Small deviations are noticed around some of the maxima, but these are of minor importance from an engineering point of view. The present example clearly shows that the two-component representation (9) in terms of the undamped mode and the mode obtained by locking the damper gives a very accurate description of the actual damped vibration mode. And the simple formula in Eq. (26) is a very efficient means for finding the modal damping properties of a discrete structure with external damper.

The explicit solution is presented in the figure by the full lines, where (———) represents viscous damping, while (– – –) and (· · · · · ·) represent damping by the first- and second-order filters, respectively. The explicit format leads to semi-circular frequency loci, where the radius increases with the phase angle. It was demonstrated in Ref. [11] that this format leads to sufficiently accurate solutions for viscous damping. The present analysis clearly shows that in general the explicit solution is only representative for moderate damping, as for modes 2–4 in case 2. For more aggressive control, like for the modes in case 1 below the cut-off frequency, the exact frequency loci do not follow semi-circular paths. In these situations the modal damping properties should be determined by the iterative procedure based on formula (26).

8. Conclusions

The objective of the present paper is to discuss and illustrate the possible increase in damping efficiency that can be obtained by active control with a damper force that operates ahead of velocity. The analysis is based on the modal properties of the damped system. The damper characteristics are represented by a frequency dependent transfer function and a damper gain. The simple two-component representation of the damped vibration mode leads simple solutions for the natural frequency. It is demonstrated that this representation is actually very accurate, even for large damping effects. And due to the general representation of the damper properties this solution can be applied to numerous linear damper models of passive and active type. The present analysis clearly indicates that attainable damping might be increased by reducing the apparent stiffness component of the damper. For active control this means that negative stiffness might lead to a significant increase in efficiency. This has been illustrated by an example with an energy radiation condition for a cable, where ideal damping by an impedance condition requires a significant negative stiffness component, which exactly eliminates the inherent structural stiffness at the location of the damper. Negative stiffness corresponds to phase lead, and therefore to a damper force that acts ahead of velocity. Desirable phase lead might easily be implemented by simple linear filters with low-pass properties. These filters are constructed so that phase lead in the low-frequency range leads to large damping for the modes below cut-off, while vanishing magnitude in the high-frequency range reduces the possibility of noise amplification. The improvement in damping efficiency that can be obtained by active control with phase lead is finally illustrated by a numerical example. It compares the damping efficiency of the filter models with that of pure viscous damping, and it turns out that in the frequency range, where the phase lead is substantial, the active models are significantly better. The numerical example also demonstrates the remarkable accuracy of the closed form solutions for the natural frequency.

Acknowledgments

This work has been supported by the Danish Technical Research Council via the project ‘Damping Mechanisms in Dynamics of Structures and Materials’.

References

[1] T.T. Soong, G.F. Dargush, *Passive Energy Dissipation Systems in Structural Engineering*, Wiley, Chichester, 1997.
[2] L. Meirovitch, *Dynamics and Control of Structures*, Wiley, New York, 1990.
[3] M.J. Balas, Feedback control of flexible structures, *IEEE Transactions on Automatic Control* 23 (4) (1978) 673–679.
[4] A. Preumont, *Vibration Control of Active Structures*: *An Introduction*, second ed., Kluwer, Dordrecht, 2002.
[5] M.J. Balas, Direct velocity feedback control of large space structures, *Journal of Guidance, Control and Dynamics* 2 (1979) 252–253.
[6] F. Bossens, Amortissement Actif des Structures Câblées: De la Théorie à L’implémentation, Ph.D. Thesis, Université Libre de Bruxelles, 2001 (in French).
[7] Y. Achkire, A. Preumont, Active tendon control of cable-stayed bridges, *Earthquake Engineering and Structural Dynamics* 25 (6) (1996) 585–597.
[8] C.J. Goh, T.K. Caughey, On the stability problem caused by finite actuator dynamics in the collocated control of large space structures, *International Journal of Control* 41 (3) (1985) 787–802.
[9] E. Sim, S.W. Lee, Active vibration control of flexible structures with acceleration feedback, *Journal of Guidance, Control and Dynamics* 16 (2) (1993) 413–415.

[10] M. Geradin, D. Rixen, *Mechanical Vibrations*, second ed., Wiley, Chichester, 1997.
[11] J.A. Main, S. Krenk, Efficiency and tuning of viscous dampers on discrete systems, *Journal of Sound and Vibration* 286 (2005) 97–122.
[12] S. Krenk, Vibrations of a taut cable with an external damper, *Journal of Applied Mechanics* 67 (2000) 772–776.
[13] S. Krenk, S.R.K. Nielsen, Vibrations of a shallow cable with a viscous damper, *Proceedings of the Royal Society of London Series A* 458 (2002) 339–357.
[14] S. Krenk, Complex modes and frequencies in damped structural vibrations, *Journal of Sound and Vibration* 270 (2004) 981–996.
[15] S. Krenk, Damping mechanisms and models in structural dynamics, in: H. Grundmann, G.I. Schuëller (Eds.), *Proceedings of Structural Dynamics EURODYN2002*, Swets and Zeitlinger, Lisse, 2002, pp. 87–98.
[16] G.F. Franklin, J.D. Powell, A. Emami-Naeini, *Feedback Control of Dynamic Systems*, fourth ed., Prentice-Hall, Englewood Cliffs, NJ, 2002.
[17] S. Krenk, Frequency analysis of the tuned mass damper, *Journal of Applied Mechanics* 72 (2005) 936–942.
[18] B.R. Mace, R.W. Jones, Feedback control of flexural waves in beams, *Journal of Structural Control* 3 (1996) 89–98.
[19] C. Mei, The analysis and control of longitudinal vibrations from wave viewpoint, *Journal of Vibration and Acoustics* 124 (2002) 645–649.
[20] J.E. Luco, H.L. Wong, A. Mita, Active control of the seismic response of structures by combined use of base isolation and absorbing boundaries, *Earthquake Engineering and Structural Dynamics* 21 (1992) 525–541.
[21] J.L. Fanson, T.K. Caughey, Positive position feedback control for large space structures, *AIAA Journal* 28 (4) (1990) 717–724.